



**HAL**  
open science

## **Experimental Assessment of the Annual Growth Ring's Impact on the Mechanical Behavior of Temperate and Tropical Species**

Claude Feldman Pambou Nziengui, Jonas Turesson, Rostand Moutou Pitti, Mats Ekevad

### ► To cite this version:

Claude Feldman Pambou Nziengui, Jonas Turesson, Rostand Moutou Pitti, Mats Ekevad. Experimental Assessment of the Annual Growth Ring's Impact on the Mechanical Behavior of Temperate and Tropical Species. Bioresources, 2020. <hal-03035002>

**HAL Id: hal-03035002**

**<https://hal.science/hal-03035002v1>**

Submitted on 2 Dec 2020

HAL is a multi-disciplinary open access archive for the deposit and dissemination of scientific research documents, whether they are published or not. The documents may come from teaching and research institutions in France or abroad, or from public or private research centers.

L'archive ouverte pluridisciplinaire HAL, est destinée au dépôt et à la diffusion de documents scientifiques de niveau recherche, publiés ou non, émanant des établissements d'enseignement et de recherche français ou étrangers, des laboratoires publics ou privés.



HAL Authorization

# Experimental Assessment of the Annual Growth Ring's Impact to the Mechanical Behavior of Temperate and Tropical Species

Claude Feldman Pambou Nziengui,<sup>a,b,\*</sup> Jonas Turesson,<sup>c</sup> Rostand Moutou Pitti,<sup>a,d</sup> and Mats Ekevad<sup>c</sup>

This study presents an innovative experimental protocol linking a nondestructive (on computed tomography scanner) and destructive approach (bending test on electrostatic press). This study aims to evaluate the annual growth ring's impact on the mechanical behavior of wood. The tests were carried out on temperate specimens (*Pseudotsuga menziesii* and *Abies alba* Mill) from the Massif Central Region of France and tropical specimens (*Aucoumea klaineana* Pierre, *Milicia excelsa*, and *Pterocarpus soyauxii*) from Gabon. The connection between the mechanical parameters, taken from these tests and their structural characteristics are also highlighted. Based on these results, a database was formed of the annual growth ring's impact on the mechanical characteristics of these species. The results show that there is a link between the annual growth ring, and the mechanical and physical characteristics of the species. The number and width of the earlywood ring and its mechanical properties are also investigated for each type of species. This comparison and the link highlighted was possible due to the study of the impact of dry density's specimens, considered in this work as an adjustment parameter on the study of the mechanical behavior of these species.

**Keywords:** Tropical species; Temperate species; Congo basin forest; Massif central forest; Bending test

**Contact information:** a: Université Clermont Auvergne, CNRS, Institut Pascal, BP 10448, 63000 Clermont-Ferrand, France; b: USTM, Ecole Polytechnique de Masuku (EPM), LareVa Bois, BP 901 Franceville Gabon; c: Luleå University of Technology, Division of Wood Science and Engineering, Department of Engineering Sciences and Mathematics, Forskargatan 1, 931 87, Skellefteå, Sweden; d: CENAREST, IRT, BP 14070, Libreville, Gabon; \*Corresponding author: pclaudefeldman@gmail.com

## INTRODUCTION

Predicting the behavior of wood under mechanical or environmental stress is essential to improve the design and durability of timber structures (Gérard et al. 2011). This refers to the understanding of the various physical and mechanical characteristics of wood. This understanding is affected by the multitude of climates encountered throughout the world, which attribute to each species endemic characteristics proper to the environment in which the species is found (Manfoumbi Boussougou 2012). One explanation of these intrinsic characteristics could be given by the anatomical structure for each species (Fig. 1).

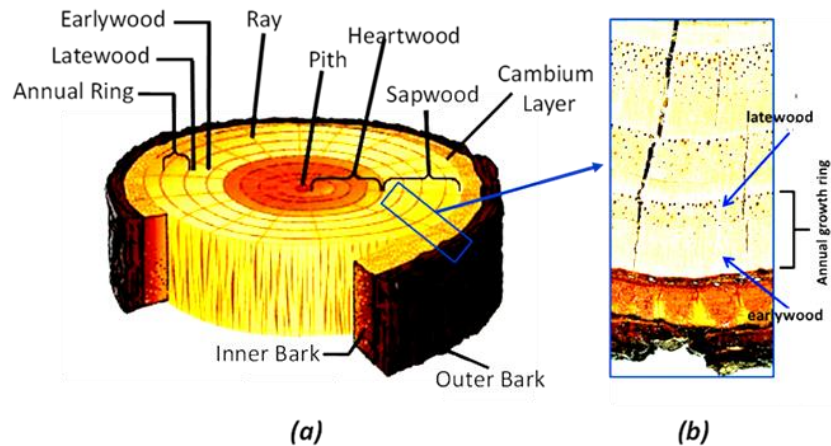


Fig. 1. (a) Cross-section of a tree trunk and (b) annual growth ring of wood

The microscale structure in wood globally affects its mechanical behavior. This can be investigated due to advancements in theoretical, numerical, and experimental approaches. Gershon *et al.* (2010) have shown that it is necessary to know the microscale structure of palmetto wood to be able to optimize its fracture toughness. Another work on palmetto wood (Saavedra Flores 2016) explains that there are influences of several micro-structural features (such as cellulose content and its crystallinity, the microfibril angle, and the cell-wall thickness of micro-fibers) on the Young modulus and density. The growth of annual rings affects the mechanical behavior of wood (Miksic 2013). Wood is a heterogeneous, anisotropic, and hygroscopic natural composite material, with high strength and stiffness relative to its weight (Mishnaevsky and Qing 2008; Bahar 2019). By starting from these hypotheses, Stanzl-Tschegg (2006) noted that the structure of wood is highly optimized for the needs of living trees. This does not mean that wood is optimized for usage in constructions where this article is focusing. The study by Morales-Conde and Machado (2017) assesses the cross-section for variation of timber bending of modulus of elasticity and brings more information linked to our work. The authors show, despite the stress waves approach used, a great correlation between the cross-sectional variation and the modulus of elasticity of the wood studied, which roughly fits with the aims of this study. Based on previous studies (Jaskowska-Lemańska and Wałach 2016; Ramage *et al.* 2017; Zeller *et al.* 2017; Abdelmohsen *et al.* 2018), it is logical to say that the mechanical behavior of wood is based on its micro-structural features, for example content of cellulose, fibril angles, and the annual growth rings.

This work aims at performing an experimental comparative study on five species with different physico-mechanical characteristics. The study is made possible due to a specific experimental approach built by connecting annual growth rings with global mechanical behavior by determining their intrinsic mechanical characteristics. Five species were studied: two European temperate species from the Massif Central in France, Douglas fir (*Pseudotsuga menziesii*) and White fir (*Abies alba* Mill); and three tropical species from Gabon, Okume (*Aucoumea klaineana* Pierre), Iroko (*Milicia excelsa*) and Padouk (*Pterocarpus soyauxii*). The difference between the chosen species is the climate of their habitat. In Gabon, for example, the climate shows a mean annual rainfall of 1900 mm, a mean relative humidity of 85%, and mean annual temperature of 27 °C (Medzegue *et al.* 2007; Pambou Nziengui *et al.* 2017; Engonga Edzang *et al.* 2020). This kind of region has two types of seasons: a six months' dry season and a six months' rainy season.

88 During the dry season, almost no rainfall occurs in comparison to the rainy season when  
 89 most of the rainfall occurs. Thus, the quantity of water absorbed by the tree during the  
 90 rainy season becomes very important for the growth of the tree.

91 To date, no study has compared tropical species (African tropical region) and  
 92 temperate species regarding the link between the growth of annual rings and the  
 93 mechanical properties. The reason for this concern is that the tropical species has a  
 94 continuous growth of annual rings during the year (Manfoumbi Boussougou 2012;  
 95 Ramage *et al.* 2017) and this is not the case for the studied temperate species. Both the  
 96 tropical and temperate species are commonly used in structure for heavy and light  
 97 frameworks, glulam, paper pulp, fiber panels, in cooperage, packaging, maritime work,  
 98 and luxury furniture (Adamopoulos 2009; Treml and Jeske 2012; Sopushynskyy 2017).  
 99 In France there were more than 170 Mm<sup>3</sup> of white fir and 93 Mm<sup>3</sup> of Douglas fir in 2009  
 100 (Pambou Nziengui *et al.* 2019). The chosen tropical species are the most widespread  
 101 species in the tropical forest of Gabon and also among the most exported and used  
 102 species in the field of timber structures (Odounga *et al.* 2018).

## 105 EXPERIMENTAL

### 107 Wood specimens

108 The wood specimens were cuboid shaped with the approximately dimensions of  
 109 200×10×10 mm<sup>3</sup> (Fig. 2). These specimens were cut following the fiber direction (in the  
 110 longest direction). A total of 125 clear wood specimens was obtained. The specimens of  
 111 temperate species were taken from collapsed beams used in an earlier study of creep tests  
 112 (Pambou Nziengui *et al.* 2019; Tran *et al.* 2018). The specimens of tropical species were  
 113 cut from butt logs at an approximate position of one meter above the roots of the standing  
 114 tree (Odounga *et al.* 2018). To equalize the moisture content (MC) of the specimens, the  
 115 specimens were stored in a climate chamber for 48 h. The temperature and the relative  
 116 humidity in the climate chamber were set to 20 °C and 64.7%, respectively. Table 1  
 117 shows the total number of specimens and the statistical mean of the principal physical  
 118 characteristics for each group before the experimental campaign.

120 **Table 1.** Number of Specimens and Physical Characteristics for Each Tested  
 121 Species Group with Coefficient of Variation (COV) in Parentheses

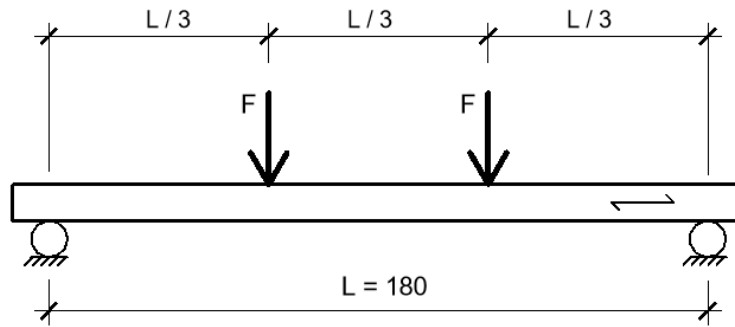
|           | Species     | Name     | No. | $MC_{mean}$ [%] | $\rho_{dry, mean}$ [kg/m <sup>3</sup> ] |
|-----------|-------------|----------|-----|-----------------|---|
| Temperate | Douglas fir | DF       | 30  | 9.8 (11.1%)     | 563 (4.5%)                              |
|           | White fir   | WF       | 48  | 9.9 (13.6%)     | 447 (8.1%)                              |
| Tropical  | Iroko       | <i>I</i> | 17  | 9.0 (17.8%)     | 582 (13.8%)                             |
|           | Padouk      | <i>P</i> | 15  | 8.3 (13.4%)     | 733 (3.0%)                              |
|           | Okume       | <i>O</i> | 15  | 10.3 (15.7%)    | 505 (4.1%)                              |

122 No.: number of specimens;  $MC_{mean}$ : mean moisture content;  $\rho_{dry, mean}$ : mean dry density

124 To distinguish the earlywood and latewood, which make up the annual growth  
 125 ring, the specimens were scanned in a computed tomography scanner (CT-scanner). The  
 126 data from the CT-scanner was visualized and analyzed by the Image J software  
 127 (<https://imagej.nih.gov/ij/>).

### 129 Four-points flexural test

130 All specimens were loaded in four-point flexural test until failure by an  
 131 electrostatic press (Fig. 2). The four-point bending test set-up was performed according to  
 132 the European requirement (EN 1995-1-1 2004) and as presented by (Manfoumbi  
 133 Boussougou 2012). The specimens were measured and weighed to determine their  
 134 physical parameters (Table 1).  
 135



136  
 137

138 **Fig. 2.** Four-point flexural test set-up with the fiber direction of the specimen loaded  
 139

140 The modulus of elasticity (MOE) was calculated for each specimen according to  
 141 Eq. 1,

$$142 \quad MOE = \frac{23L^3}{648I_z \left( 2 \frac{F_2 - F_1}{W_2 - W_1} - \frac{2L}{5Gbh} \right)} \quad (1)$$

143 where  $F_2 - F_1$  is an increase of force on the regression line and  $W_2 - W_1$  is the increase of  
 144 the corresponding displacement as described in the European standard requirement (EN  
 145 1995-1-1 2004).  $L$  represents the distance between the two supports (Fig. 2),  $I_z$  the  
 146 moment of inertia,  $G$  is the shear modulus,  $b$  and  $h$  are the width and height of the  
 147 specimen, respectively. Due to lack of data for the tropical species, the influence of  $G$   
 148 was neglected. The maximum flexural stress was defined to Eq. 2,

$$149 \quad C_{max} = M_y / I_z \quad (2)$$

150 where  $M$  is the flexural moment at the maximum force,  $F_{max}$ , during the four-point  
 151 flexural test,  $y$  is the distance from the neutral axis to the area of highest flexural moment  
 152 and  $I_z$  the moment of inertia. For this four-point flexural test set-up,  $M$  was calculated as  
 153 presented by Eq. 3,

$$154 \quad M = (LF_{max}) / 3 \quad (3)$$

155 To calculate  $C_{max}$ , the length  $y$  in Eq. 2 can be set equal to  $h/2$  [25]. A comparison  
 156 between  $C_{max}$  calculated in this study and the maximum flexural failure stress given by  
 157 the CIRAD wood collection (Gérard et al. 2011),  $C_{mcir}$ , was done.  
 158  
 159

## 160 RESULTS AND DISCUSSION

161

### 162 Mechanical Characterization of the Specimens in Static Tests

163 The mean values of modulus of elasticity ( $MOE$ ), maximum loading ( $F_{max}$ ), and  
 164 maximum flexural stress ( $C_{max}$ ) obtained, for each species studied, are presented in Table  
 165 2. The  $C_{mcir}$  value is the maximum flexural stress given by the CIRAD wood collection

166 (Gérard *et al.* 2011). The highest  $MOE_{mean}$  of 15.6 GPa was obtained for DF species. The  
 167 lowest  $MOE_{mean}$  of 9.2 GPa was calculated for O. The lowest and highest  $F_{max}$ , mean was  
 168 measured for WF and DF, respectively and the specimens with largest variation among  
 169 the tropical and temperate species was P and DF, respectively. By taking into account the  
 170 results of (Gérard *et al.* 2011) and its dry density (Table 1), P was expected to have the  
 171 highest  $C_{max}$  mean among all tested species, but according to Table 2, it had a lower  $C_{max}$   
 172 mean but with the highest  $COV$ . In general, all tested species (except WF and P) had a  
 173 higher  $C_{max}$ , mean than  $C_{mcir}$ . These results highlight the intra-extra trees variability,  
 174 which exists for specimens taken from the same trees.

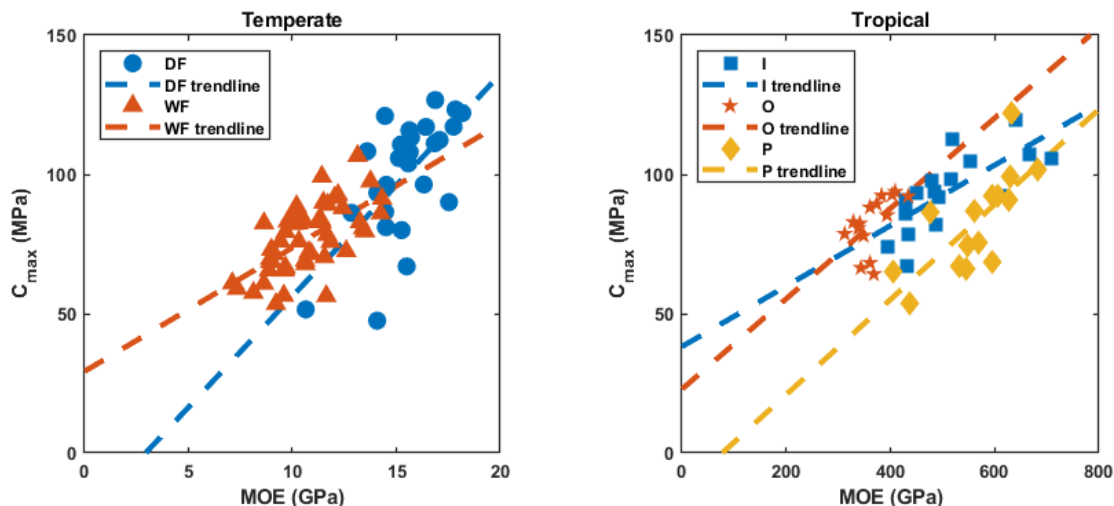
175  
 176

**Table 2.** Result from the Four-Point Flexural Test with  $COV$  in Parentheses

|           | Name | $MOE_{mean}$ (GPa) | $F_{max, mean}$ (N) | $C_{max, mean}$ (MPa) | $C_{mcir}$ (MPa) |
|-----------|------|--------------------|---------------------|-----------------------|------------------|
| Temperate | DF   | 15.6 (10.5%)       | 522 (20.7%)         | 102 (20.4%)           | 91               |
|           | WF   | 10.7 (16.4%)       | 383 (15.3%)         | 77 (16.0%)            | 80               |
| Tropical  | I    | 12.8 (18.1%)       | 492 (13.7%)         | 94 (14.8%)            | 87               |
|           | P    | 14.1 (13.5%)       | 407 (21.6%)         | 83 (21.5%)            | 116              |
|           | O    | 9.2 (9.1%)         | 422 (12.7%)         | 82 (11.9%)            | 62               |

177  
 178  
 179  
 180  
 181  
 182  
 183  
 184  
 185  
 186

Figure 3 shows the evolutions of the  $C_{max}$  versus  $MOE$  for all tested specimens. There was an increasing  $C_{max}$  for a higher  $MOE$ . This behavior is observable for the both temperate and tropical specimens. The difference in  $COV$ , which exists for the groups of specimens presented in Table 2 is also visible in Fig. 3 by the highlighting of the dispersion, which seems large for DF (for the temperate specimens) and P (for tropical specimens). The groups of specimens with lower  $COV$  (O and WF) showed a non-scattering pattern in Fig. 3 compared to groups of specimens with higher  $COV$ . The  $R^2$ -values for the trendlines were calculated as 0.41, 0.41, 0.53, 0.30, and 0.53 for DF, WF, I, O, and P, respectively.

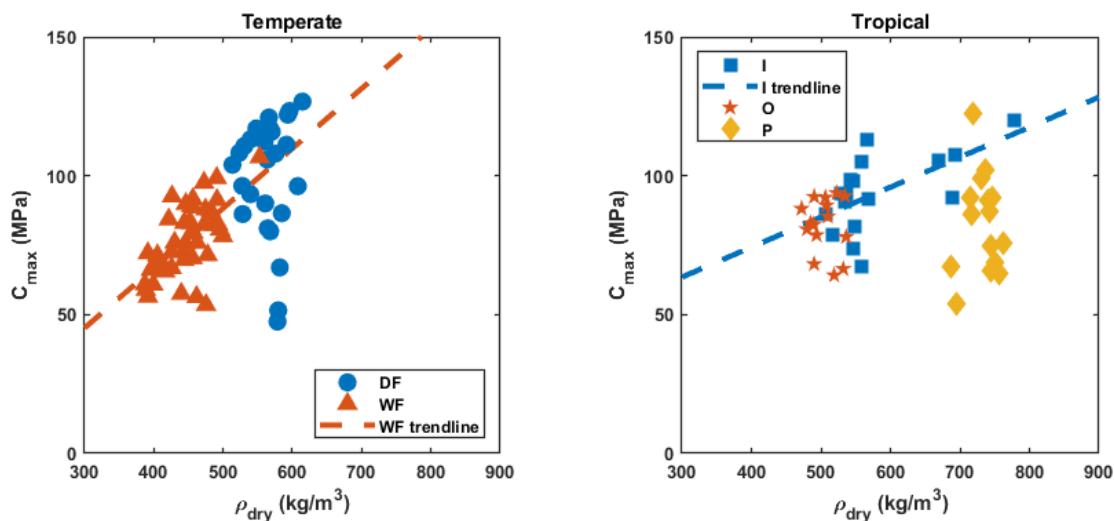


187  
 188  
 189  
 190  
 191  
 192  
 193

**Fig. 4.** Modulus of elasticity ( $MOE$ ) versus maximum flexural stress ( $C_{max}$ ) for the groups of temperate and tropical specimens

Figure 4 shows a comparison between the  $\rho_{dry}$  and  $C_{max}$ . Due to the low  $COV$  for the  $\rho_{dry}$  of the DF, the DF specimens are non-scattered. The lower values of  $C_{max}$  for some DF specimens occur due to material variations. The DF specimens with lower  $C_{max}$  were

194 kept in the analysis because they could not be classified as statistical outliers. The results  
 195 for the temperate specimens were similar for the tropical specimens where the group of  
 196 specimens with highest  $COV$  could illustrate a trendline with reasonable  $R^2$ -values. The  
 197 trendlines in Fig. 4 had an  $R^2$ -value of 0.40 and 0.35 for WF and I, respectively. The  
 198 other temperate and tropical specimens resulted in trendlines with low  $R^2$ -values and are  
 199 not presented. Iroko (I) was the only tropical group of specimens following a trendline. O  
 200 and P did not illustrate a trendline due to the low  $COV$  of  $\rho_{dry}$ , which were 4.1% and  
 201 3.0%, respectively. This variation in  $\rho_{dry}$  was too low compared to the  $COV$  of  $\rho_{dry}$  for I  
 202 and WF, which were 13.8% and 8.1%, respectively. This statistical study done on the  
 203 intrinsic mechanical characteristics of the specimens from temperate and tropical species,  
 204 gives interesting information to build a database of the mechanical properties of the  
 205 species studied. This database will be important for the next sections of this work.  
 206

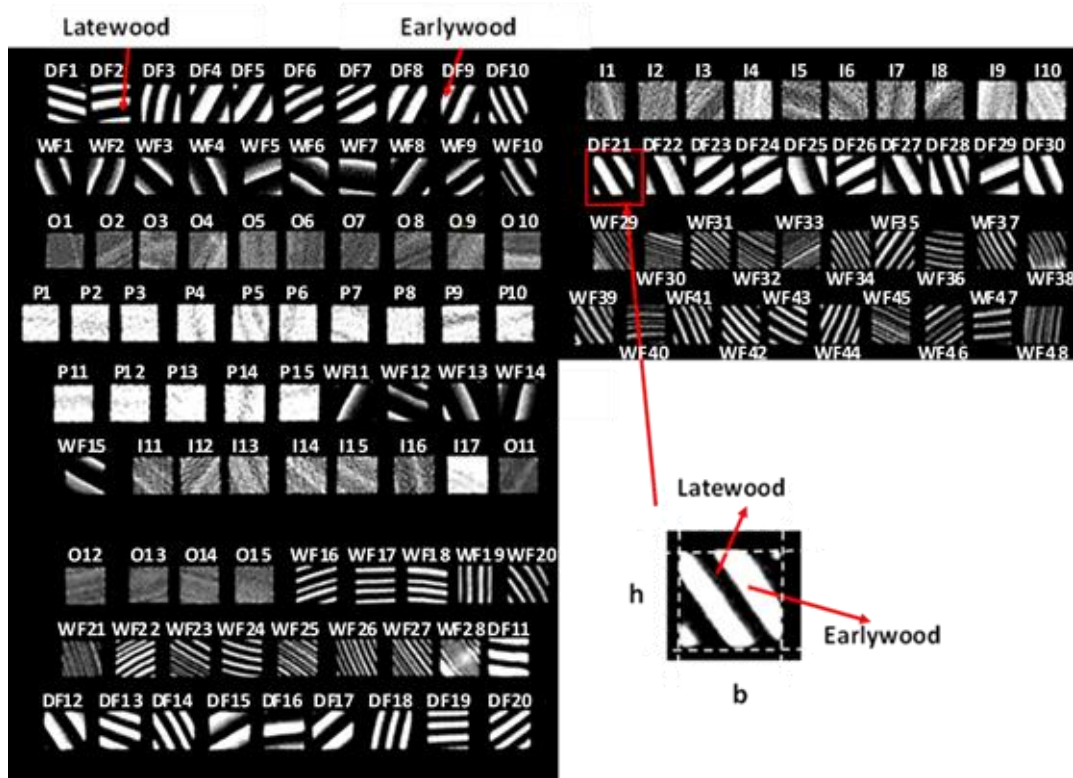


207  
 208 **Fig. 5.** Dry density ( $\rho_{dry}$ ) versus maximum flexural stress ( $C_{max}$ ) for the groups of temperate and  
 209 tropical specimens  
 210

### 211 Cross-section Characterization of the Specimens

212 The CT scans of specimens cross-sections are presented in Fig. 5. The earlywood  
 213 and latewood, which make up the annual growth ring of tree, are illustrated with white  
 214 and black color, respectively. The distinction between earlywood and latewood is easily  
 215 observable for the temperate specimens (Fig. 5, DF and WF species), but on the cross  
 216 sections of the tropical specimens, the distinction of annual growth ring is almost  
 217 impossible to see (Fig. 5; O, I and P species). These observations are in accordance with  
 218 the literature (EN 1995-1-1 2004; Sopushynskyy *et al.* 2017), which shows that the  
 219 distinction between earlywood and latewood is therefore not obvious in tropical species.  
 220 The main explanation of the non-perception of this difference, for the tropical specimens,  
 221 could be given by the harsh climate met in the region of their growth and the fact that the  
 222 tropical species has a continuous growth of the annual rings during the year (Manfoumbi  
 223 Boussougou 2012; Ramage *et al.* 2017). Specifically, for the P specimens the distinction  
 224 between the lines of latewood and earlywood seems very difficult to observe, which is  
 225 the same case for O and I. In the specimens O2, O12, I3, I5 (Fig. 6), there is little  
 226 distinction observable between the latewood and earlywood of these tropical species. The  
 227 density difference through the specimen could explain the difference. By taking into  
 228 account this result, globally for the tropical species, the scanning of their cross-section

229 does not make it possible to distinguish the line between earlywood and latewood.  
 230



231  
 232 **Fig. 6.** Result from the CT-scanner with specimens named and numbered after species  
 233

234 Starting from this map (Fig. 5), Image J software was used to examine the width  
 235 of the earlywood for the temperate specimens. The results and the summary of the width  
 236 mean values of earlywood rings ( $\varpi_{mean}$ ) and the number mean values of earlywood rings  
 237 ( $NE_{mean}$ ) are presented in Table 3. The tropical specimens had a lower  $NE_{mean}$  than the  
 238 temperate specimens. Lowest number of  $NE_{mean}$  of 1.9 had P. For the tropical specimens,  
 239 O had the highest  $NE_{mean}$  and  $COV$ . The temperate specimens had the highest and lowest  
 240  $COV$  of 56.6% (WF) and 22.9% (DF), respectively, for the  $NE_{mean}$ . No  $\varpi_{mean}$  could not be  
 241 measured for the tropical specimens due to difficulty of define where earlywood starts and  
 242 latewood ends (see Fig. 5 for specimens of species I, P, and O).  
 243

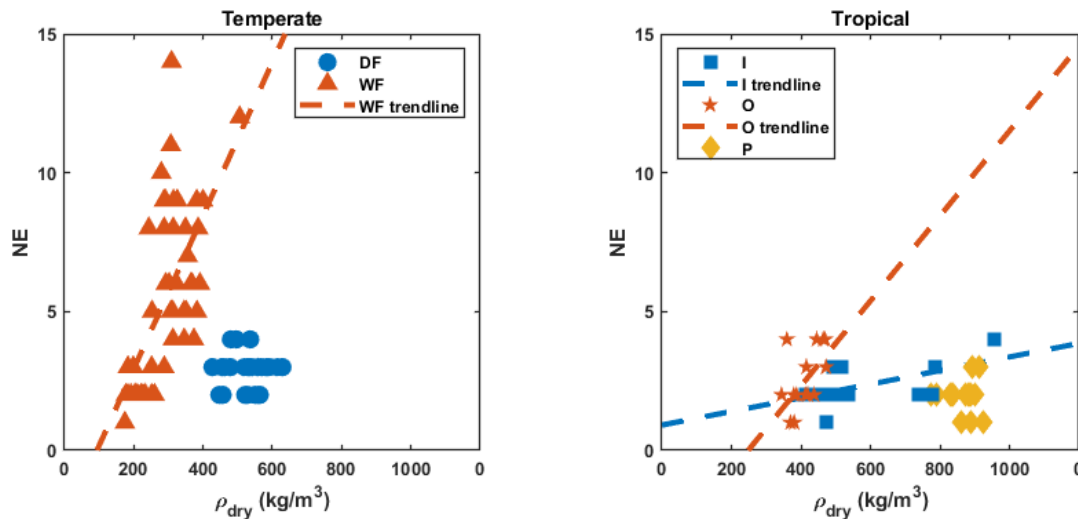
244 **Table 3.** Mean Width ( $\varpi_{mean}$ ) and Number of Earlywood Rings ( $NE_{mean}$ ) for the  
 245 Groups of Tropical and Temperate Specimens with  $COV$  in Parentheses

|           | Name | $\varpi_{mean}$ [mm] | $NE_{mean}$ |
|-----------|------|----------------------|-------------|
| Temperate | DF   | 5.07 (31.4%)         | 2.8 (22.9%) |
|           | WF   | 3.37 (69.6%)         | 5.5 (56.6%) |
| Tropical  | I    | -                    | 2.3 (29.9%) |
|           | P    | -                    | 1.9 (30.7%) |
|           | O    | -                    | 2.5 (45.6%) |

246  
 247 **Assessment of the Annual Growth Ring in the Mechanical Properties of the**  
 248 **Species Studied**

249 To understand the effects of the annual growth ring on the mechanical behavior,

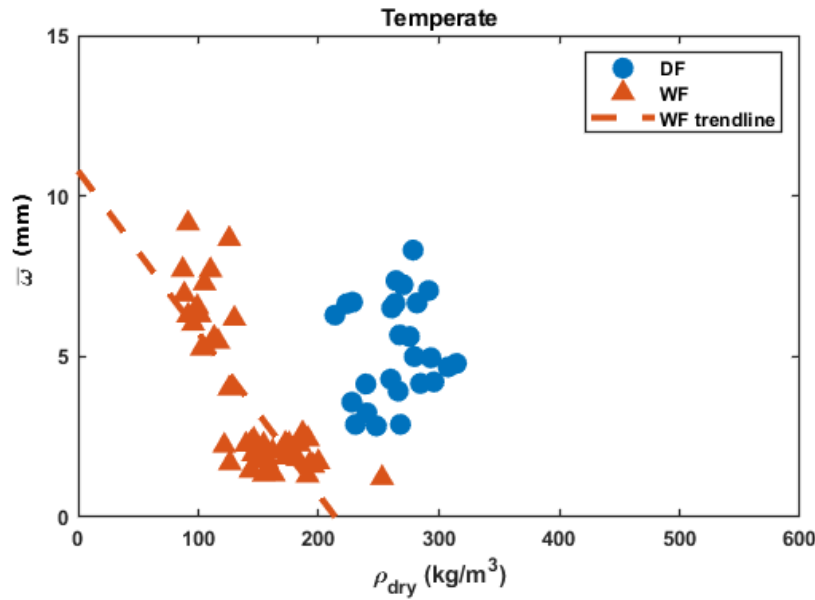
250 comparisons were made between the  $\rho_{dry}$  and NE (Fig. 6) and the  $\rho_{dry}$  and  $\varpi$  (Fig. 7).  
 251



252  
 253 **Fig. 7.** Dry density ( $\rho_{dry}$ ) versus the number of earlywood rings ( $NE$ ) for the groups of temperate  
 254 and tropical specimens

255  
 256 The temperate specimens show that there was a correlation between the  $\rho_{dry}$  and  
 257  $NE$ . This conclusion was drawn only from the WF specimens and not the DF specimens  
 258 due to the DF specimens low  $COV$  of 22.9%. For the tropical specimens, a correlation  
 259 between  $\rho_{dry}$  and  $NE$  is difficult to see due to the low spread of the specimens. The  
 260 illustrated trendlines for the tropical specimens had lower  $R^2$ -values of 0.30 and 0.32 for I  
 261 and O, respectively, compared to the  $R^2$ -value of 0.40 for WF. The tropical trendlines  
 262 was showing a positive correlation between  $\rho_{dry}$  and  $NE$  but due to the lower  $R^2$  values,  
 263 the trend is not as clear as for the temperate specimens. For the group of DF specimens  
 264 and the group of P specimens trendlines were not presented due to the low  $R^2$ -values.

265 The correlation between the  $\rho_{dry}$  versus  $\varpi$  for the temperate specimens is  
 266 presented in Fig. 7. A negative correlation between  $\rho_{dry}$  and  $\varpi$  could be seen for the WF  
 267 specimens. Due to the low  $COV$  of 22.9% and 31.4% for  $\rho_{dry}$  and  $\varpi$ , respectively, for the  
 268 DF specimens it was not possible to see any correlation between  $\rho_{dry}$  and  $\varpi$ . The trendline  
 269 for the group of WF specimens had an  $R^2$ -value of 0.60. A trendline for the group of DF  
 270 specimens was not presented due to the low  $R^2$ -value.  
 271



272  
273 **Fig. 8.** Dry density ( $\rho_{dry}$ ) versus the width of earlywood rings ( $\varpi$ ) for the groups of temperate  
274 specimens  
275

276  
277 **CONCLUSIONS**

- 278  
279 1. An experimental study of the evaluation of the annual growth ring impact on the  
280 intrinsic physico-mechanical characteristics of wood has been done. The samples  
281 were dimensioned and tested in a four-point flexural test according to the European  
282 standard requirement. Two groups of specimens have been studied (temperate and  
283 tropical species). To be able to visualize the earlywood and latewood (annual growth  
284 ring), the specimens were scanned by a computed tomography scanner before the  
285 four-point flexural test.
- 286 2. The results show that, for temperate species, the distinction between earlywood and  
287 latewood make up the annual growth ring and is easily distinguishable. However, for  
288 a tropical species the distinction is less clear. The study shows trendlines for the  
289 temperate and tropical specimens connecting the modulus of elasticity to the  
290 maximum flexural stress. It was also possible to show a trendline between the dry  
291 density and the maximum flexural stress for the two groups of temperate and tropical  
292 specimens of White fir and Iroko, respectively. Another trendline was shown between  
293 the dry density and number of earlywood rings for the group of temperate specimens  
294 of White fir and the groups of tropical specimens of Iroko and Okume. A last  
295 trendline was shown between the dry density and the mean width of the earlywood  
296 rings for the group of temperate specimens of White fir. The mean width of the  
297 earlywood rings was not possible to measure for the groups of tropical specimens due  
298 to the difficulty of define exactly where earlywood starts and latewood ends.
- 299 3. The results showed a connection between the annual growth rings of the tree and their  
300 intrinsic physico-mechanical characteristics mainly based on the dry density of the  
301 wood for both the tropical and temperate specimens. It was possible to show that the  
302 dry density was affected by the number and width of the earlywood rings. Moreover,  
303 the dry density affected the maximum flexural stress and where the maximum

304 flexural stress is strongly connected to the modulus of elasticity. This results in an  
305 increased number of earlywood rings which then results in an increased modulus of  
306 elasticity and increased maximum flexural stress. These results illustrate the need to  
307 have a fairly large number of specimens to avoid the large variation noted within the  
308 mechanical properties determined in this work. These results are interesting but are  
309 limited by the fact that it is a new experimental approach used for this type of study.  
310 It could be necessary for the next experimental study to create a method to distinguish  
311 clearly the annual growth rings of tropical species by increasing, for example, the size  
312 of the samples to be studied.

313

314

## 315 ACKNOWLEDGMENTS

316

317 The authors would like to thank Luleå University of Technology in Skellefteå,  
318 Sweden, including the Wood Science and Engineering Division of the Department of  
319 Engineering and Mathematics for the provision of study materials. The authors also thank  
320 the TOR Program of the French Embassy in Sweden which allowed the initial  
321 collaboration but also the ANR for the financial support of this work through the project  
322 CLIMBOIS N ° ANR-13-JS09-0003-01 labeled ViaMeca. And finally, the authors thank  
323 the CNRS, which partly supported this work through the PEPS project "Green  
324 Engineering" RUMO and Region AURA thanks to SCUSI Project.

325

326

## 327 REFERENCE CITED

328

- 329 Abdelmohsen, S., Adriaenssens, S., El-Dabaa, R., Gabriele, S., Olivieri, L., and Teresi, L.  
330 (2019). "A multi-physics approach for modeling hygroscopic behavior in wood low-  
331 tech architectural adaptive systems," *Computer-Aided Design* 106, 43-53. DOI:  
332 10.1016/j.cad.2018.07.005
- 333 Adamopoulos, S., Milios, E., Doganos, D., and Bistinas, I. (2009). "Ring width, latewood  
334 proportion and dry density in stems of *Pinus brutia* Ten. ," *European Journal of*  
335 *Wood and Wood Products* 67(4), 471. DOI: 10.1007/s00107-009-0345-x
- 336 Bahar, R., Ouertani, S., Azzouz, S., Naili, H., El Ayeb, M. T., and El Cafci, A. (2019).  
337 "Mechanical properties changes in oak (*Quercus canariensis*) and stone pine (*Pinus*  
338 *pinea*) wood subjected to various convective drying conditions," *European Journal of*  
339 *Environmental and Civil Engineering* 1–13. DOI: 10.1080/19648189.2018.1500308
- 340 Brancheriau, L., Kouchade, C., and Brémaud, I. (2010). "Internal friction measurement of  
341 tropical species by various acoustic methods," *J. Wood Sci.* 56(5), 371–379.
- 342 EN 1995-1-1 (2004). "1-1 Eurocode 5: Design of timber structures," European  
343 Committee for Standardization, Brussels, Belgium.
- 344 Engonga Edzang, A. C., Pambou Nziengui, C. F., Ekomy Ango, S., Ikogou, S., and  
345 Moutou Pitti, R. (2020). "Comparative studies of three tropical wood species under  
346 compressive cyclic loading and moisture content changes," *Wood Material Science &*  
347 *Engineering* 1-8. DOI : 10.1080/17480272.2020.1712739
- 348 Gérard, J., Guibal, D., Paradis, D., Vernay, M., Beauchêne, J., Brancheriau, L., Châlon,  
349 I., Daigremont, C., Détienne, P., Fouquet, D., Langbour, P., Lotte, S., Thévenon, M-  
350 F., Méjean, C., and Thibaut, A. (2011). *Tropix 7*. CIRAD. DOI:

- 351 10.18167/74726f706978  
352 Gershon, A. L., Bruck, H. A., Xu, S., Sutton, M. A. and Tiwari, V. (2010). “Multiscale  
353 mechanical and structural characterizations of Palmetto wood for bio-inspired  
354 hierarchically structured polymer composites,” *Materials Science and Engineering C*  
355 30(2), 235-244. DOI: 10.1016/j.msec.2009.10.004  
356 Jaskowska-Lemańska, J., and Wałach, D. (2016). “Impact of the direction of non-  
357 destructive test with respect to the annual growth rings of pine wood,” *Procedia*  
358 *Engineering* 161, 925-930. DOI: 10.1016/j.proeng.2016.08.761  
359 Manfoumbi Boussougou, N. (2012). Contribution à l’Adaptation de l’Eurocode 5 Aux  
360 Essences Tropicales Dans Leur Environnement, Thesis, Univ. Limoges, France.  
361 Medzegue, M. J., Grelier, S., Bertrand, M., Nziengui, M., and Stokes, A. (2007). “Radial  
362 growth and characterization of juvenile and adult wood in plantation grown okoumé  
363 (*Aucoumea klaineana* Pierre) from Gabon,” *Annals of Forest Science* 64(8), 815-824.  
364 DOI: 10.1051/forest:2007065  
365 Miksic, A., Myntti, M., Koivisto, J., Salminen, L., and Alava, M. (2013). “Effect of  
366 fatigue and annual rings’ orientation on mechanical properties of wood under cross-  
367 grain uniaxial compression,” *Wood Science and Technology* 47(6), 1117-1133. DOI:  
368 10.1007/s00226-013-0561-8  
369 Mishnaevsky, L., and Qing, H. (2008). “Micromechanical modelling of mechanical  
370 behaviour and strength of wood: State-of-the-art review,” *Computational*  
371 *Materials Science* 44(2), 363-370. DOI: 10.1016/j.commatsci.2008.03.043  
372 Morales-Conde, M. J., and Machado, J. S. (2017). “Evaluation of cross-sectional  
373 variation of timber bending modulus of elasticity by stress waves,” *Construction and*  
374 *Building Materials* 134, 617-625. DOI: 10.1016/j.conbuildmat.2016.12.188  
375 Odounga, B., Pitti, R. M., Toussaint, E., and Grédiac, M. (2018). “Mode I fracture of  
376 tropical woods using grid method,” *Theoretical and Applied Fracture Mechanics* 95,  
377 1-17. DOI: 10.1016/j.tafmec.2018.02.006  
378 Pambou Nziengui, C. F., Ikogou, S., and Moutou Pitti, R. (2018). “Impact of cyclic  
379 compressive loading and moisture content on the mechanical behavior of *Aucoumea*  
380 *klaineana* Pierre,” *Wood Material Science & Engineering* 13(4), 190-196. DOI:  
381 10.1080/17480272.2017.1307281  
382 Pambou Nziengui, C. F., Moutou Pitti, R., Fournely, E., Gril, J., Godi, G., and Ikogou, S.  
383 (2019). “Notched-beam creep of Douglas fir and white fir in outdoor conditions:  
384 Experimental study,” *Construction and Building Materials* 196, 659-671. DOI:  
385 10.1016/j.conbuildmat.2018.11.139  
386 Ramage, M. H., Burrige, H., Busse-Wicher, M., Fereday, G., Reynolds, T., Shah, D. U.,  
387 Wu, G., Yu, L., Fleming, P., Densley-Tingley, D., and Allwood, J. (2017). “The  
388 wood from the trees: The use of timber in construction,” *Renewable and Sustainable*  
389 *Energy Reviews* 68, 333-359. DOI: 10.1016/j.rser.2016.09.107  
390 Saavedra Flores, E. I., and Haldar, S. (2016). “Micro–macro mechanical relations in  
391 Palmetto wood by numerical homogenisation,” *Composite Structures* 154, 1-10. DOI:  
392 10.1016/j.compstruct.2016.06.050  
393 Sopushynskyy, I., Kharyton, I., Teischinger, A., Mayevskyy, V., and Hrynyk, H. (2017).  
394 “Wood density and annual growth variability of *Picea abies* (L.) Karst. growing in  
395 the Ukrainian Carpathians,” *European Journal of Wood and Wood Products* 75(3),  
396 419-428. DOI: 10.1007/s00107-016-1079-1  
397 Stanzl-Tschegg, S. E. (2006). “Microstructure and fracture mechanical response of  
398 wood,” *International Journal of Fracture* 139(3–4), 495-508. DOI: 10.1007/s10704-

- 399 006-0052-0  
400 Timoshenko, P. S. (1968). *Résistance des matériaux*. Résistance des matériaux. Dunod,  
401 Paris, <https://cds.cern.ch/record/111473>  
402 Tran, T. B., Bastidas-Arteaga, E., Aoues, Y., Pambou Nziengui, C. F., Hamdi, S. E.,  
403 Moutou Pitti, R., Fournely, E., Schoefs F., and Chateauneuf, A. (2018). “Reliability  
404 assessment and updating of notched timber components subjected to environmental  
405 and mechanical loading,” *Engineering Structures* 166, 107-116. DOI:  
406 10.1016/j.engstruct.2018.03.053  
407 Treml, S., and Jeske, H. (2012). “Splinter formation of OSB strands during flat disc  
408 cutting of ring porous hardwoods,” *European Journal of Wood and Wood Products*  
409 70(1-3), 293-297. DOI: 10.1007/s00107-011-0559-6  
410 Zeller, L., Ammer, C., Annighöfer, P., Biber, P., Marshall, J., Schütze, G., del Río  
411 Gaztelurrutia and Pretzsch, H. (2017). “Tree ring wood density of Scots pine and  
412 European beech lower in mixed-species stands compared with monocultures,” *Forest  
413 Ecology and Management* 400, 363-374. DOI: 10.1016/j.foreco.2017.06.018  
414  
415 Article submitted: February 24, 2020;